

Speed Synchronization of web winding System with Sliding Mode Control

Hachemi Glaoui, Abdeldejbar Hazzab, Bousmaha Bouchiba, Ismaïl Khalil Bousserhane

Laboratory of command Analysis and Optimization of the Electro-Energizing Systems, Faculty of Sciences and technology, BECHAR University B.P. 417 BECHAR, 08000

Article Info

Article history:

Received Jan 16, 2013

Revised Apr 23, 2013

Accepted May 17, 2013

Keyword:

Winding system

Induction motor Proportional-Integral (PI)

Sliding mode control SISO

Sliding mode control MIMO

ABSTRACT

A continuous web winding system is a large-scale, complex interconnected dynamic system with numerous tension zones to transport the web while processing it. There are two control schemes for large-scale system control: the centralized scheme and the decentralized scheme. Centralized control is the traditional control method, which considers all the information about the system to be a single dynamic model and design a control system for this model. A speed synchronization control strategy for multiple induction motors, based on adjacent cross-coupling control structure, is developed by employing total sliding mode control method. The proposed control strategy is to stabilize speed tracking of each induction motor while synchronizing its speed with the speed of the other motors so as to make speed synchronization error amongst induction motors converge to zero. The global stability and the convergence of the designed controller are proved by using Lyapunov method. Simulation results demonstrate the effectiveness of the proposed method.

Copyright © 2013 Institute of Advanced Engineering and Science.
All rights reserved.

Corresponding Author:

Hachemi Glaoui,

Faculty of Sciences and technology, BECHAR University B.P. 417 BECHAR, 08000

Email: mekka60@gmail.com

1. INTRODUCTION

Web winding systems are common in the manufacture, fabrication, and transport of any materials such as paper, metal, and photographic film. A continuous web processing line is a large-scale, complex interconnected dynamic system with numerous tension zones to transport the web while processing it. A continuous web processing line is also a web transporting system which consists of a combination of some basic mechanical/electrical elements, such as unwinder, rewinder, roller, free web span, measuring sensors, and driving motors.

With the rapid development of modern manufacturing, a challenging problem in modern induction motor control field is that the motion of multiple motors must be controlled in a synchronous manner, for instance of distributed papermaking machines, continuous rolling mills, print works, and spinning works. The performance of synchronization control affects the reliability and precision of product seriously [1]. In multiple-motor applications, the synchronization performance of the system may be degraded by many factors such as disturbances in the load and system parameters variation due to environmental changes [2–3], thus high performance synchronization control of multiple induction motors is important in practice.

In this article, total sliding mode control is adopted in adjacent cross-coupling control structure to implement speed synchronization of multiple induction motors. The speed synchronization strategy is to stabilize synchronization errors between each motor and the other two motors to zero.

The tracking error controllers and the synchronization error controllers both include an equivalent control law and a robust control law, which makes the stable tracking performances and synchronization performances are ensured against the system uncertainties. Simulations on a five motor system are given, and

the performance of the proposed control strategy in several typical working conditions has been studied. Lyapunov stability analysis and simulation results demonstrate the effectiveness of the proposed control strategy.

2. SYSTEM MODELS

In the mechanical part, the motor M1 carries out unreeling, M3 drives the fabric by friction and M5 is used to carry out winding, each one of the motors M2 and M4 drives two rollers via gears “to grip” the band (Figure 1). Each one of M2 and M4 could be replaced by two motors, which each one would drive a roller of the stages of pinching off. The elements of control of pressure between the rollers are not represented and not even considered in the study. The stage of pinching off can make it possible to isolate two zones and to create a buffer zone. [8, 9].

The objective of these systems is to maintain the tape speed constant and to control the tension in the band.

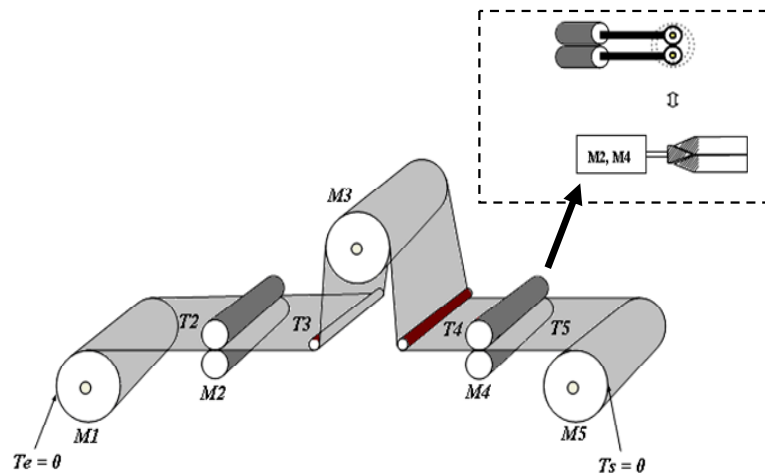


Figure1. Five motors web transport system

The used motor is a three phase induction motor type (IM) supplied by an inverter voltage controlled with Pulse Modulation Width (PWM) techniques. A model based on circuit equivalent equations is generally sufficient in order to make control synthesis. The dynamic model of three-phase, Y-connected induction motor can be expressed in the d-q synchronously rotating frame as [13]:

$$\begin{cases}
 \frac{di_{ds}}{dt} = \frac{1}{\sigma L_s} \left(- \left(R_s + \left(\frac{L_m}{L_r} \right)^2 R_r \right) i_{ds} + \sigma L_s \omega_e i_{qs} + \frac{L_m R_r}{L_r^2} \phi_{dr} + \frac{L_m}{L_r} \phi_{qr} \omega_r + V_{ds} \right) \\
 \frac{di_{qs}}{dt} = \frac{1}{\sigma L_s} \left(- \sigma L_s \omega_e i_{ds} - \left(R_s + \left(\frac{L_m}{L_r} \right)^2 R_r \right) i_{qs} - \frac{L_m}{L_r} \phi_{dr} \omega_r + \frac{L_m R_r}{L_r^2} \phi_{qr} + V_{qs} \right) \\
 \frac{d\phi_{dr}}{dt} = \frac{L_m R_r}{L_r} i_{ds} - \frac{R_r}{L_r} \phi_{dr} + (\omega_e - \omega_r) \phi_{dr} \\
 \frac{d\phi_{qr}}{dt} = \frac{L_m R_r}{L_r} i_{qs} - (\omega_e - \omega_r) \phi_{dr} - \frac{R_r}{L_r} \phi_{qr} \\
 \frac{d\omega_r}{dt} = \frac{P^2 L_m}{L_r J} (i_{qs} \phi_{dr} - i_{ds} \phi_{qr}) - \frac{f_c}{J} \omega_r - \frac{P}{J} T_l
 \end{cases} \quad (1)$$

Where σ is the coefficient of dispersion and is given by:

$$\sigma = 1 - \frac{L_m^2}{L_s L_r} \quad (2)$$

The tension model in web transport systems is based on Hooke's law, Coulomb's law, [8, 9] mass conservation law and the laws of motion for each rotating roll.

A. Hooke's law

The tension T of an elastic web is function of the web strain ε

$$T = ES \varepsilon = ES \frac{L - L_0}{L_0} \quad (3)$$

Where E is the Young modulus, S is the web section, L is the web length under stress and L_0 is the nominal web length (when no stress is applied).

B. Coulomb's law

The study of a web tension on a roll can be considered as a problem of friction between solids, see [8] and [9]. On

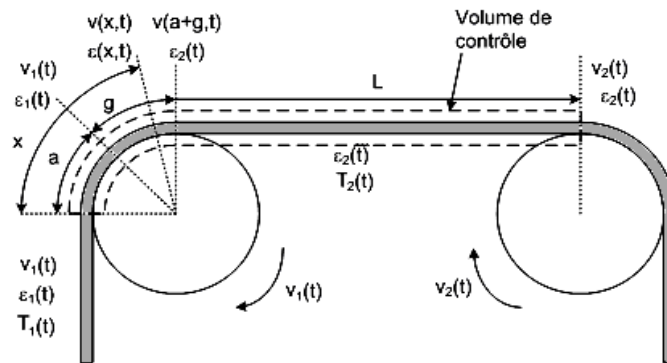


Figure2. Web tension on the roll

The roll, the web tension is constant on a sticking zone of arc length a and varies on a sliding zone of arc length g (cf. Figure 2, where $V_k(t)$ is the linear velocity of the roll k). The web tension between the first contact point of a roll and the first contact point of the following roll is given by:

$$\begin{aligned} \varepsilon(x, t) &= \varepsilon_1(t) & \text{if } x \leq a \\ \varepsilon(x, t) &= \varepsilon_1(t) e^{\mu(x-a)} & \text{if } a \leq x \leq a + g \\ \varepsilon(x, t) &= \varepsilon_2(t) & \text{if } a + g \leq x \leq L_t \end{aligned}$$

Where μ is the friction coefficient, And $L_t = a + g + L$. The tension change occurs on the sliding zone. The web velocity is equal to the roll velocity on the sticking zone.

C. Mass conservation law

Consider an element of web of length $L = L_0(1 + \varepsilon)$

With a weight density ρ , under an unidirectional stress. The cross section is supposed to be constant. According to the mass conservation law, the mass of the web remains constant between the state without stress and the state with stress

$$\rho SL = \rho_0 SL_0 \Rightarrow \frac{\rho}{\rho_0} = \frac{1}{1 + \varepsilon} \quad (4)$$

D. Tension model between two consecutive rolls

The equation of continuity, cf. [8], applied to the web gives:

$$\frac{\partial \rho}{\partial t} + \frac{\partial (\rho V)}{\partial x} = 0 \quad (5)$$

By integrating on the variable x from 0 to Lt (cf. Figure 2), taking into account (4), and using the fact that $a + g \ll L$, we obtain

$$\frac{d}{dt} \left(\frac{L}{1 + \varepsilon_2} \right) = \frac{V_1}{1 + \varepsilon_1} - \frac{V_2}{1 + \varepsilon_2}.$$

Therefore:

$$-L \frac{d\varepsilon_2}{dt} = V_1 \frac{(1 + \varepsilon_2)^2}{1 + \varepsilon_1} - V_2 (1 + \varepsilon_2). \quad (6)$$

This equation can be simplified by using the approximation

$$\varepsilon_1 \ll 1 \quad \text{and} \quad \varepsilon_2 \ll 1 \quad \frac{(1 + \varepsilon_2)^2}{1 + \varepsilon_1} \approx (1 - \varepsilon_1)(1 + 2\varepsilon_2) \quad (7)$$

And using Hook's law, we get:

$$L_{k-1} \frac{dT_k}{dt} \cong ES(V_k - V_{k-1}) + T_{k-1}V_{k-1} - T_k(2V_{k-1} - V_k). \quad (8)$$

$k = 2, 3, 4, 5.$

Where L_{k-1} is the web length between roll $k-1$ and roll k , T_k is the tension on the web between roll $k-1$ and roll k , V_k is the linear velocity of the web on roll k , Ω_k is the rotational speed of roll k , R_k is the radius of roll k , E is the Young modulus and S is the web section.

E. Roll velocity calculation

The law of motion can be obtained with a torque balance:

$$\frac{d(J_k \Omega_k)}{dt} = R_k (T_{k+1} - T_k) + Cem_k + C_f \quad (9)$$

Where $\Omega_k = V_k / R_k$, is the rotational speed of roll k Cem_k is the motor torque (if the roll is driven) and C_f is the friction torque.

F. Complete model of the five motors system

Figure 1 shows a typical five motors system with winder, unwinder, and three tractors. The complete model of this system is given by the following equations:

$$\left\{ \begin{array}{l}
 L_1 \frac{dT_2}{dt} = ES (V_2 - V_1) - T_2 V_2. \\
 L_2 \frac{dT_3}{dt} = ES (V_3 - V_2) + T_2 V_2 - T_3 V_3. \\
 L_3 \frac{dT_4}{dt} = ES (V_4 - V_3) + T_3 V_3 - T_4 V_4. \\
 L_4 \frac{dT_5}{dt} = ES (V_5 - V_4) + T_4 V_4 - T_5 V_5. \\
 \\
 \frac{d(J_1(t)\Omega_1)}{dt} = R_1(t)T_2 + C_{em1} - f_1(t)\Omega_1. \\
 \frac{d(J_2\Omega_2)}{dt} = R_2(T_3 - T_2) + C_{em2} - f_2(t)\Omega_2. \\
 \frac{d(J_3\Omega_3)}{dt} = R_3(T_4 - T_3) + C_{em3} - f_3(t)\Omega_3. \\
 \frac{d(J_4\Omega_4)}{dt} = R_4(T_5 - T_4) + C_{em4} - f_4(t)\Omega_4.
 \end{array} \right. \quad (10)$$

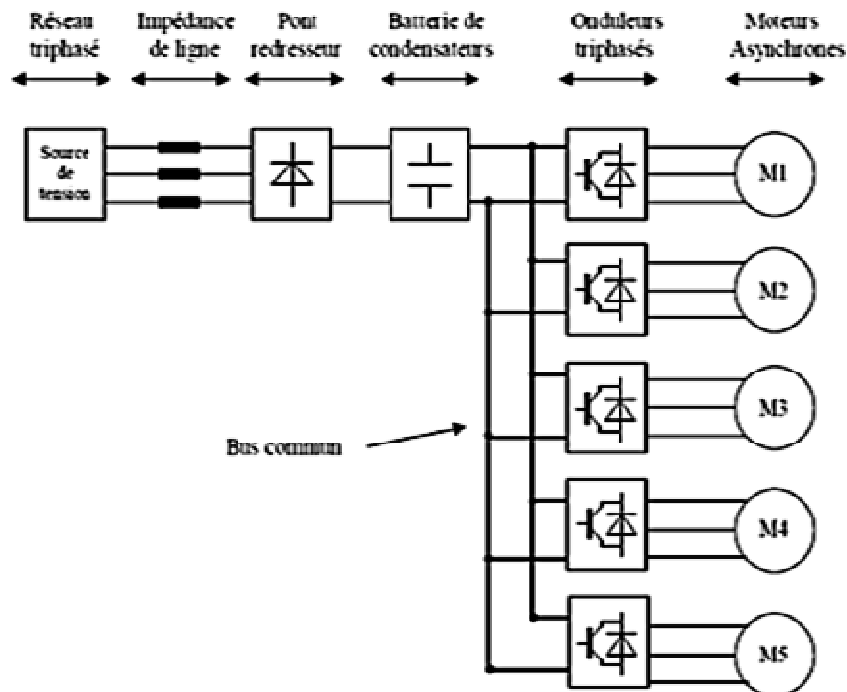


Figure 3. Electrical part of the five drive system

3. SLIDING MODE CONTROL

The sliding mode control consists in moving the state trajectory of the system toward a predetermined surface called sliding or switching surface and in maintaining it around this latter with an appropriate switching logic. In the case of the n th-order system, the sliding surface could be defined as [12]:

$$S(x) = \left(\frac{\partial}{\partial t} + \lambda \right)^{r-1} \cdot e(x) \quad (11)$$

Concerning the development of the control law, it is divided into two parts, the equivalent control U_{eq} and the attractivity or reachability control U_{sw} . The equivalent control is determined off-line with a model that represents the plant as accurately as possible. If the plant is exactly identical to the model used for determining U_{eq} and there are no disturbances, there would be no need to apply an additional control U_{sw} . However, in practice there are a lot of differences between the model and the actual plant. Therefore, the control component U_{sw} is necessary which will always guarantee that the state is attracted to the switching surface by satisfying the condition $\dot{S}(x) \cdot S(x) < 0$ [12, 13]. Therefore, the basic switching law is of the form:

$$U = U_{eq} + U_{sw} \quad (12)$$

U_{eq} is the equivalent control, and U_{sw} is the switching control. The function of U_{eq} is to maintain the trajectory on the sliding surface, and the function of U_{sw} is to guide the trajectory to this surface.

Let the sliding surface vector be given by:

$$S = [S_1 \quad S_2 \quad S_3 \quad S_4 \quad S_5]$$

With $U_{sw} = -M(S) \operatorname{sgn}(S(\cdot))$

$M(S)$: the magnitude of the attractively control law U_{sw} , and sgn : the sign function.

In a conventional variable structure control, U_{sw} generates a high control activity. It was first taken as constant, a relay function, which is very harmful to the actuators and may excite the unmodeled dynamics of the System. This is known as a chattering phenomenon. Ideally, to reach the sliding surface, the chattering phenomenon should be eliminated [12, 13]. However, in practice, chattering can only be reduced.

The first approach to reduce chattering was to introduce a boundary layer around the sliding surface and to use a smooth function to replace the discontinuous part of the control action as follows:

$$\begin{cases} U_{sw} = \frac{K}{\varepsilon} \cdot S(x) & \text{if } |S(x)| < \varepsilon \\ U_{sw} = K \cdot \operatorname{sgn}(S(x)) & \text{if } |S(x)| > \varepsilon \end{cases}$$

The constant K is linked to the speed of convergence towards the sliding surface of the process (the reaching mode). Compromise must be made when choosing this constant, since if K is very small the time response is important and the robustness may be lost, whereas when K is too big the chattering phenomenon increases.

4. SISO SLIDING MODE CONTROL

To control the speed of the induction machine, the sliding surface is defined as follows:

$$S(w_m) = w_m^* - w_m \quad (13)$$

The derivative of the sliding surface can be given as:

$$\dot{S}(w_m) = \dot{w}_m^* - \dot{w}_m \quad (14)$$

Taking into account the mechanical equation of the induction motor defined in the system of equations (Model), the derivative of sliding surface becomes

$$\dot{S}(w_m) = \dot{w}_m^* - \left(\frac{P^2 L_m \phi_{dr}^*}{J L_r} i_{qs} - \frac{f_c}{J} w_m - \frac{P}{J} C_r \right) \quad (15)$$

The current control is given by:

$$i_{qs}^* = i_{qseq} + i_{qs} \quad (16)$$

To avoid the chattering phenomenon produced by the *Sign* function we use the Saturation function *Sat* in the discontinuous control defined as follow:

$$sat\left(\frac{S}{\phi}\right) = \begin{cases} \frac{S}{\phi} & ; \quad \text{if} \quad \left| \frac{S}{\phi} \right| < 1 \\ \text{Sign}\left(\frac{S}{\phi}\right) & ; \quad \text{if} \quad \left| \frac{S}{\phi} \right| > 1 \end{cases} \quad (17)$$

Where ϕ is the boundary layer thickness.

The discontinuous control action can be given as:

$$i_{qs}^n = k_{iqs} \cdot sat(s(\omega)/\phi_\omega) \quad (18)$$

k_{iqs} : Positive constant.

$$i_{qseq} = \frac{J L_r}{P^2 L_m \phi_{dr}^*} \left(\dot{w}_m^* + \frac{f_c}{J} w_m + \frac{P}{J} C_r \right) \quad (19)$$

The Figure 4 shows the SMC control strategy scheme for each induction motor.

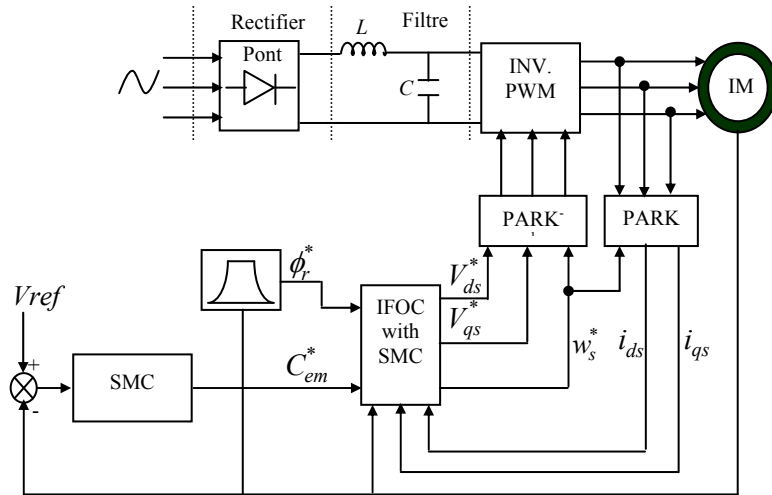


Figure 4: Block diagram for each motor with SMC control

$$S_1 = i_{ds}^* - i_{ds} \tag{20}$$

$$S_2 = i_{qs}^* - i_{qs} \tag{21}$$

The derivate of S_1 can be given as:

$$\dot{S}_1 = \dot{i}_{ds}^* - \dot{i}_{ds}$$

From equation (1) and (14) we can obtain :

$$\dot{S}_1 = \dot{i}_{ds}^* - \left(-\frac{1}{\sigma L_s} \left(R_s + R_r \left(\frac{L_m}{L_r} \right)^2 \right) i_{ds} + \omega_s \cdot i_{qs} + \frac{L_m \cdot R_r}{\sigma L_s L_r^2} \cdot \phi_r^* + \frac{1}{\sigma L_s} V_{ds} \right) \tag{22}$$

The virtual voltage controller V_{ds} is given by:

$$V_{ds}^* = V_{dseq} + V_{dsn} \tag{23}$$

The voltage discontinuous control V_{qsn} is defined as:

$$V_{dsn} = k_1 \cdot \text{sat}(s_1 / \phi_1) \tag{24}$$

According to Lyapunov stability criteria [10], our speed loop system's stable if: $S_1 \dot{S}_1 < 0$ by means that K_1 is positive constant.

The equivalent control V_{dseq} is given as:

$$V_{dseq} = \sigma L_s \left(\dot{i}_{ds}^* + \frac{1}{\sigma L_s} \left(R_s + R_r \left(\frac{L_m}{L_r} \right)^2 \right) i_{ds} - \omega_s \cdot i_{qs} - \frac{L_m \cdot R_r}{\sigma L_s L_r^2} \phi_r^* \right) \tag{25}$$

The derivate of S_2 can be given as:

$$\dot{S}_2 = \dot{i}_{qs}^* - \dot{i}_{qs} \tag{26}$$

From equation (16) and (26) we can obtain:

$$\dot{S}_2(i_{qs}) = \dot{i}_{qs}^* - (-\omega_s i_{ds} - \frac{1}{\sigma L_s} \left(R_s + R_r \cdot \left(\frac{L_m}{L_r} \right)^2 \right) i_{qs} - \frac{L_m}{\sigma L_s L_r} \cdot \dot{\phi}_r^* \cdot \omega_m + \frac{1}{\sigma L_s} V_{qs}) \tag{27}$$

The voltage controller V_{qs} is given by:

$$V_{qs}^* = V_{qseq} + V_{qsn} \tag{28}$$

The V_{qseq} equivalent control actions defined as:

$$V_{qseq} = \sigma \cdot L_s \cdot (i_{qs}^* \lim + \omega_s \cdot i_{ds} + \frac{1}{\sigma \cdot L_s} \left(R_s + R_r \cdot \left(\frac{L_m}{L_r} \right)^2 \right) i_{qs} + \frac{L_m}{\sigma L_s L_r} \cdot \dot{\phi}_r^* \cdot \omega_m) \tag{29}$$

The voltage discontinuous control V_{dsn} is defined as:

$$V_{qsn} = k_2 \cdot \text{sat}(s_2 / \phi_2) \tag{30}$$

For the same reason condition of K_1, K_2 are positives constant

5. MIMO SLIDING MODE CONTROL

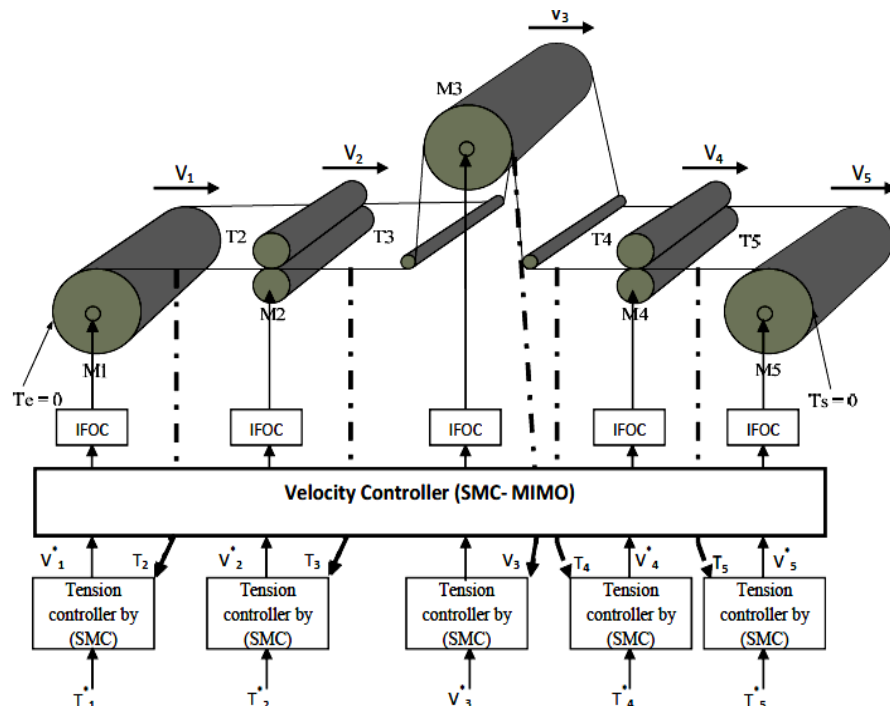


Figure 5. Block diagram for multi motors web winding system with MIMO-SMC control.

We consider a multi variable defined in the state space as follows:

$$\dot{x}_n = Ax(t) + Bu(t)$$

u is a vector of dimension (r), ($u = [u_1 \ u_2 \ \dots \ u_r]^T$)

$$\begin{aligned} \dot{x}_n &= [x_1^{n1} \ x_2^{n2} \ \dots \ x_i^{ni} \ \dots \ x_m^{nm}]^T \\ A &= [f_{n1} \ f_{n2} \ \dots \ f_{ni} \ \dots \ f_{nm}]^T \\ B &= [b_{ij}] = [b_{ij}], \text{ et} \end{aligned}$$

$$x = \underbrace{[x_1 \ x_1^{(1)} \ x_1^{(n1-1)}]}_{nm} \ \dots \ \underbrace{[x_i \ x_i^{(1)} \ x_i^{(ni-1)}]}_{ni} \ \dots \ \underbrace{[x_m \ x_m^{(1)} \ x_m^{(nm-1)}]}_{ni}^T$$

The vector of the surface is the same size as the control vector;

$$S = [S_1 \ S_2 \ \dots \ S_r]$$

It can be written as follows;

$$\dot{S}(x) = F(t, x) + D(t, x)U \tag{31}$$

$F(t, x)$: is a vector of dimension (r)

$D(t, x)$: is a square matrix ($r \times r$)

$$U_{eq}(x, t) = -D(t, x)^{-1} F(t, x)$$

$$U_n(x, t) = -\alpha_i \text{Sat}(S^*(x))$$

$$S^*(x) = D^t(t, x)S(x)$$

Where denotes the vector

$$\alpha_i = \begin{bmatrix} \alpha_1 & 0 & 0 & \dots & 0 \\ 0 & \alpha_2 & 0 & 0 & \cdot \\ 0 & 0 & \alpha_3 & 0 & 0 \\ \cdot & 0 & 0 & \dots & 0 \\ \cdot & \cdot & \cdot & \cdot & \cdot \\ 0 & 0 & 0 & 0 & \alpha_5 \end{bmatrix} \text{ Et } \alpha_i > 0$$

$$F(x,t) = \begin{bmatrix} \left(\frac{1}{R_1(t)} \cdot \frac{dR_1(t)}{dt} - \frac{1}{J_1(t)} \cdot \frac{dJ_1(t)}{dt} - \frac{f_{e1}(t)}{J_1(t)} \right) \cdot V_1 + \frac{R_1^2(t)}{J_1(t)} \cdot (T_2) \\ \left(\frac{1}{R_2(t)} \cdot \frac{dR_2(t)}{dt} - \frac{1}{J_2(t)} \cdot \frac{dJ_2(t)}{dt} - \frac{f_{e2}(t)}{J_2(t)} \right) \cdot V_2 + \frac{R_2^2(t)}{J_2(t)} \cdot (T_3 - T_2) \\ \left(\frac{1}{R_3(t)} \cdot \frac{dR_3(t)}{dt} - \frac{1}{J_3(t)} \cdot \frac{dJ_3(t)}{dt} - \frac{f_{e3}(t)}{J_3(t)} \right) \cdot V_3 + \frac{R_3^2(t)}{J_3(t)} \cdot (T_4 - T_3) \\ \left(\frac{1}{R_4(t)} \cdot \frac{dR_4(t)}{dt} - \frac{1}{J_4(t)} \cdot \frac{dJ_4(t)}{dt} - \frac{f_{e4}(t)}{J_4(t)} \right) \cdot V_4 + \frac{R_4^2(t)}{J_4(t)} \cdot (T_5 - T_4) \\ \left(\frac{1}{R_5(t)} \cdot \frac{dR_5(t)}{dt} - \frac{1}{J_5(t)} \cdot \frac{dJ_5(t)}{dt} - \frac{f_{e5}(t)}{J_5(t)} \right) \cdot V_5 + \frac{R_5^2(t)}{J_5(t)} \cdot (-T_5) \end{bmatrix}$$

$$D(x,t) = \begin{bmatrix} R_1(t)J_1(t) & 0 & 0 & 0 & 0 \\ 0 & R_2(t)J_2(t) & 0 & 0 & 0 \\ 0 & 0 & R_3(t)J_3(t) & 0 & 0 \\ 0 & 0 & 0 & R_4(t)J_4(t) & 0 \\ 0 & 0 & 0 & 0 & R_5(t)J_5(t) \end{bmatrix}$$

The surface S_i is given by:

$$S_i = V_i^* - V_i \quad \text{With } i = 1, 2, 3, 4, 5$$

The derivative of the surface is: $\dot{S}_i = \dot{V}_i^* - \dot{V}_i$

$$\left\{ \begin{array}{l} \dot{S}_1 = \dot{V}_1^* - \dot{V}_1 \\ \dot{S}_2 = \dot{V}_2^* - \dot{V}_2 \\ \dot{S}_3 = \dot{V}_3^* - \dot{V}_3 \\ \dot{S}_4 = \dot{V}_4^* - \dot{V}_4 \\ \dot{S}_5 = \dot{V}_5^* - \dot{V}_5 \end{array} \right.$$

6. SIMULATION RESULTS

The winding system we modeled is simulated using MATLAB SIMULINK software and the simulation is carried out on 2s.

To evaluate system performance we carried out numerical simulations under the following Conditions:

- Start with the linear velocity of the web of 5m / s.
- The motor M1 has the role of Unwinder a roll radius R1 (R1 = 2.25 m).
- The motors M2, M3, M4 are the role is to pinch the tape.
- The motor M5 has the role of winding a roll of radius R5. The aims of the STOP block is to stop at the same time the different motors of the system when a radius adjust to a desired value (for example R5 = 0.8 m), by injecting a reference speed zero.

As shown in Figure (6-8). An improvement of the linear speed is registered, and has follows the reference speed for both PI controller and SMC control, but in case of PI controller, the overshoot in linear speed of Unwinder is 25%. Figure (7) and Figure (8) show that with the SMC MIMO controller the system follows the reference speed after 0.8 sec, in all motors, however, in the SMC SISO and PI controller the system follows after 1.5 sec and 2 sec respectively.

1. Comparison of the control performances: it has been made by the comparison of the average speeds of the five motors V_{avg} , for each controller this average is expressed by the equation (32).
2. Comparison of synchronism between the speeds of the five motors: in this point one makes a comparison between the deviation standard of speeds of five motors V_{std} , for each controller this average is expressed by the equation (33).

$$V_{avg} = \frac{1}{n} \sum_{i=1}^n V_i \quad (32)$$

$$V_{std} = \left(\frac{1}{n} \sum_{i=1}^n (V_i - V_{avg})^2 \right)^{\frac{1}{2}} \quad (33)$$

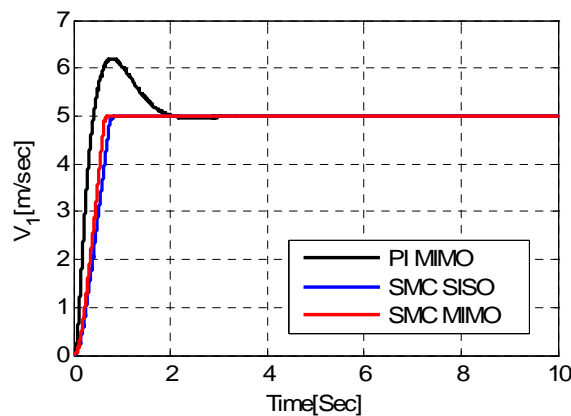


Figure 6: The linear speed of unwinder M1

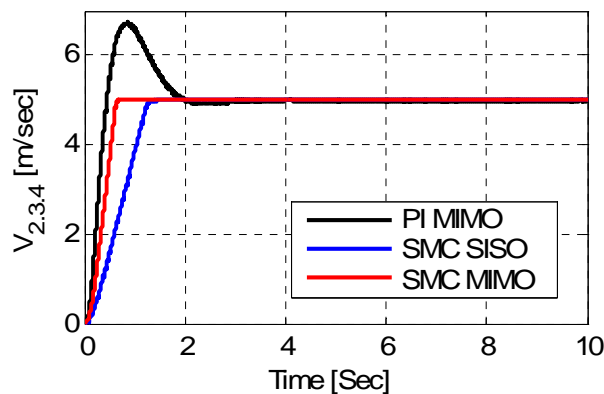


Figure 7: The linear speed of motors M2, M3 and M4

From the figures (6-8), we can say that: the effect of the disturbance is neglected in the case of the SMC MIMO controller. It appears clearly that the classical control with PI controller is easy to apply. However the

control with sliding mode MIMO controllers offers better performances in both of the overshoot control and the tracking error.

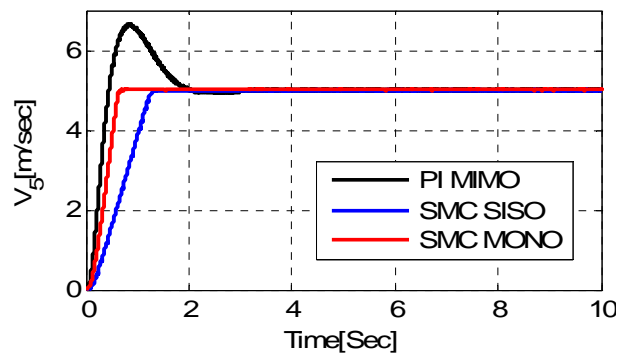


Figure 8. The linear speed of winder M5

Figure (9) and Figure (10) shows the comparison between the SMC-MIMO controller, the SMC-SISO controller and the PI- MIMO controller. After this comparison we can judge that the SMC-MIMO controller presents a clean improvement to the level of the performances of control, compared to the PI-MIMO controller, the synchronism between the five motors is improved with SMC-MIMO controller compared to SMC-SISO controller.

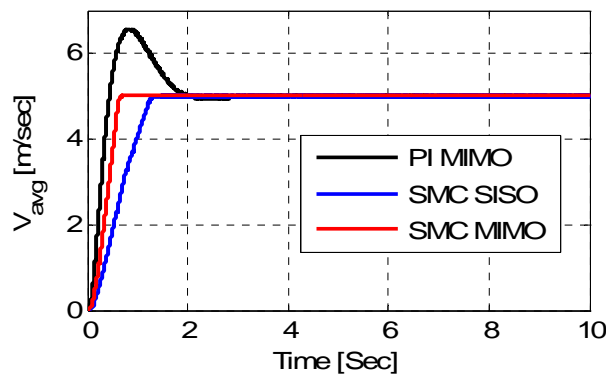


Figure 9: comparison between the SMC MIMO, SMC SISO and PI MIMO with average speeds of five motors

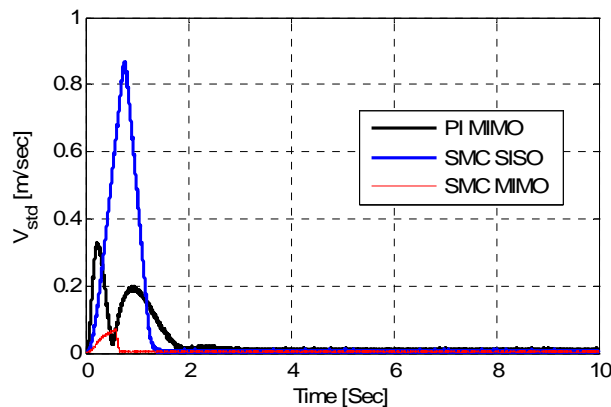


Figure 10: comparison between the SMC MIMO, SMC SISO and PI MIMO with the deviation standard of speeds of five motors

7. CONCLUSION

A new synchronization control strategy of multiple induction motors is proposed in this article sliding mode control of the field oriented induction motor was proposed. To show the effectiveness and performances of the developed control scheme, simulation study was carried out. Good results were obtained despite the simplicity of the chosen sliding surfaces. The robustness and the tracking qualities of the proposed control system using sliding mode controllers appear clearly.

The objective of this paper consists in developing a model of a winding system constituted of five motors that is coupled mechanically by a strap whose tension is adjustable and to develop the methods of analysis and synthesis of the commands robust and their application to synchronize the five sequences and to maintain a constant mechanical tension between the rollers of the system.

The simulations results show the efficiency of the SMC-MIMO controller technique, however the strategy of SMC-MIMO Controller brings good performances, and she is more efficient than the SMC-SISO controller and classical PI-MIMO controller.

REFERENCES

- [1] Christian Thiffault Pierre Sicard Alain Bouscayrol. TENSION CONTROL LOOP USING A LINEAR ACTUATOR BASED ON THE ENERGETIC MACROSCOPIC REPRESENTATION *CCECE 2004- CCGEI 2004*, Niagara Falls, May/mai 2004
- [2] S Charlemagne, A Bouscayrol, Slama-Belkhodja, JP Hautier. "Flatness based control of non-linear textile multimachine process". in Proc. of EPE'03, CD-ROM, Toulouse (France), September 2003.
- [3] Adlane Benlatreche Dominique Knittel. "State Feedback Control with Full or Partial Integral Action for Large Scale Winding Systems". *Industry Applications Conference, 2005*. Vol. 2 page(s): 973- 978 Oct 2005
- [4] Boubaker, R M'hiri, M Ksouri, JP Babary. "MIMO variable structure control for non linear distributed parameter systems: application to fixed bed bioreactors". IEEE CESA'98, Nabeul-Hammamet (Tunisia), MACS Multiconfaence, Symposium on Modelling, Analysis and Control. vol 1, 1-4
- [5] Boubaker, R M'hiri, M Ksouri, JP Babary. "SISO and MIMO variable structure control of fixed bed bioreactors". *UKAC Internationnal Conference CONTRL'98, Vol. 1,,IEE Conference Publication no 455*, London, Swansea (UK). 1-4 September 1998, pp. 229-234. April 1998, pp.79-84.
- [6] JP Babary 8z S Boml. "Sliding mode control of a denitrifying Biofilter". to be published in *Applied Mathematical Modelling*.
- [7] Rahmi Guclu. "Sliding mode and PID control of a structural system against earthquake". *Mathematical and Computer Modelling*. 44 (2006) 210–217
- [8] G Brandenburg. "Ein mathematisches Modell fur eine durchlaufende elastische Stoffbahn in einem System angetriebener, umschlungener, Walzen". *Regelungstechnik und Prozess-Datenverarbeitung*. vol.3:69–162,1973.
- [9] H Koc. "Modelisation et commande robuste d'un system d'entrainement de bande flexible". Ph.D. thesis, Universite Louis Pasteur (Strasbourg I University), 2000.
- [10] J Jung, K Nam. "A Dynamic Decoupling Control Scheme for High-Speed Operation of Induction Motors". *IEEE Trans. on Ind. Elect.* Vol. 46/01 (1999).
- [11] A Mezouar, MK Fellah, SHadjeri. "Adaptive Sliding Mode Observer for Induction Motor Using Two-Time Scale Aproach". *Electric Power Research* 16.2008.1323-1336.
- [12] RJ Wai. "Adaptive Sliding-Mode Control for Induction Servomotor Drives". *IEE Proc. Elecrr. Power Appl.* 2000,147, pp. 553-562.
- [13] M Zhiwen, T Zheng, F Lin and X You. "a New Sliding-Mode Current Controller for Field Oriented Controlled Induction Motor Drives". *IEEE Int. Conf. IAS (2005)*. pp. 1341-1346, 2005.
- [14] Wai RJ, Lin KM, Lin CY. "Total sliding-mode speed control of field-oriented induction motor servo drive". *Proceedings of the 5th Asian Control Conference*. 2004: 1354–1361.

BIOGRAPHIES OF AUTHORS



Hachemi Glaoui*- was born in 1977 at Bechar-Algeria, he's received the electrical engineering diploma from Bechar University,-Algeria in 2001, and the Master degree from the University Bechar Algeria in 2008. Currently, he is an assistant professor at Bechar University.
Ph.d. degree in multi machine system control.
E-mail: glaouih@yahoo.fr



Hazzab Abdeldjabar - received the state engineer degree in electrical engineering in 1995 from the University of Sciences and Technology of Oran (USTO), Algeria the M.Sc. degree from the Electrical Engineering Institute of the USTO in 1999. and the Ph.D. degree from the Electrical Engineering Institute of the USTO in 2006. He is currently professor of electrical engineering at University of Bechar, Algeria, where he is Director of the Research Laboratory of Control Analysis and Optimization of the Electro-Energetic Systems. His research interests include power electronics, electric drives control, and artificial intelligence and their applications. Professor of electrical engineering at University of Bechar, Algeria.



Bouchiba Bousmaha – was born in 1977 at Bechar-Algeria, he's received the electrical engineering diploma from Bechar University,-Algeria in 1999, and the Master degree from the University Alexandria Egypt in 2006. Currently, he is an assistant professor at Bechar University.
Ph.d. degree in multi machine system control.



Ismail Khalil Bousserhane - received the B.Sc. degree in electrical engineering from the Electrical Engineering Institute of the University Center of Bechar in 2000, the M.Sc. degree in electrical engineering from the University of Sciences and Technology of Oran (USTO), Algeria, in 2003 and the Ph.D. degree from the Electrical Engineering Institute of USTO in 2008,. He is currently professor of electrical engineering at University of Béchar, Béchar, Algeria.